Research and Development Program in Reactor Diagnostics and Monitoring with Neutron Noise Methods

Stage 4. Final report

I. Pázsit and J. K-H. Karlsson

Department of Reactor Physics
Chalmers University of Technology
Göteborg 1998

Research and Development Program in Reactor Diagnostics and Monitoring with Neutron Noise Methods: Stage 4

Summary

This report gives an account of the work performed by the Department of Reactor Physics in the frame of a research contract with the Swedish Nuclear Power Inspectorate (SKI). The present work constitutes Stage 4 of a long-term research and development program concerning the development of diagnostics and monitoring methods of nuclear reactors. The long-term goals are elaborated in more detail in e.g. the Final Reports of Stage 1 and 2 (SKI Rapport 95:14 and 96:50, Refs. [1] and [2]).

Some important parts of this development program consist of modelling of the noise source, calculation of the space- and frequency dependent transfer function, calculation of the neutron noise via a convolution of the transfer function of the system and the noise source, i.e. the perturbation, and finally finding an inversion or unfolding procedure to determine noise source parameters from the neutron noise.

Most previous work is based on very simple (analytical) reactor models for the calculation of the transfer function as well as analytical unfolding methods. The purpose of this program is to abandon this restriction by calculating the transfer function in more realistic models as well as elaborating powerful inversion methods that do not require analytical transfer functions.

Concurrently with the main program, further aims of the project are to study and possibly solve certain selected reactor diagnostic problems, initiate and perform studies of theoretical problems of neutron fluctuations in nuclear systems and perform physical and simulated experiments to support the analysis of fluctuations in nuclear systems.

A further aim of the program is to build up competence within the Department of Reactor Physics, Chalmers, regarding reactor physics calculations, reactor dynamics and noise diagnostics in order to be able to solve real problems in the most effective way.

The program executed in Stage 4 consists of the following parts:

- Investigation of a non-homogeneous analytical reactor model for the calculation of neutron noise;
- Calculation and evaluation of the adiabatic approximation in the reactor model described in the previous point;
- Development of methods for the separation of concurrent global and regional power oscillations in boiling water reactors (BWRs);
- Investigation of the possibility of using the flux gradient in monitoring and diagnostics of reactor cores.

This report is based primarily on work performed by Imre Pázsit (principal investigator) and Joakim Karlsson. A proposal of items for the continuation of this program in Stage 5 is given at the end of this report.

Section 1

Investigation of models for the calculation of neutron noise

1.1 Background

In conceptual and model studies of neutron noise and diagnostics, and even in most practical applications, simple homogeneous reactor models have been used so far, in which closed form analytical solutions are possible. The reason for this is that to achieve diagnostics, i.e. unfolding of noise source properties from the induced reactor noise, an inversion of the resulting neutron noise formula is necessary. Before the advent of powerful unfolding or inversion methods such as neural networks, this was mostly possible if simple, closed form solutions of the so called direct problem, i.e. the neutron noise expressed as a function of the noise source (perturbation) could be obtained. Accordingly, in most cases investigated so far, simple homogeneous cores with or without a reflector were considered in simple 1-D or 2-D geometries, with a point, plane or line source being present.

In many practical diagnostic problems these models are too simple and more realistic models are required. We have taken a step towards less trivial models by developing an axially non-homogenous reactor model. In this model both the static flux and the noise equations can still be solved by analytical methods, and thus we retain the simplicity and convenience that closed form analytical solutions bring. Thus, a number of problems with practical relevance can be explored. These investigations and results will be reported in detail in a couple of papers ([4] and [5]).

The model consists of a 2-D homogeneous rectangular core in which a δ-function (Feinberg-Galanin) control rod is inserted partially. A sketch of the model core is shown in Fig. 1. Solution of both the static and the dynamic equations (the latter corresponding to a rod manoeuvring experiment in which the rod is moved up and down periodically) can be given by two different analytical methodologies.

First, the static problem will be investigated. The solution can in general be obtained by two different methods. One is based on a series expansion w.r.t. the eigenfunctions of the statically unperturbed system, i.e. a homogeneous system without the rod being present. However, a much more effective method is to divide the system axially into two regions, one containing the full extent of the rod and the other being the remaining part which is free of the rod. In both regions solution with separation of variables is applicable, and the solutions can be coupled to each other by interface conditions.

Second, the neutron flux fluctuations, induced by the periodic lifting and sinking of the rod (which in normal reactor operation jargon is called rod manoeuvring) will be calculated and discussed. Even in this case, both above mentioned solution methods can be used. Actually this perturbation can be represented by a point source at the rod edge. However, this point source is acting in a static system which is axially non-homogeneous and this fact makes the problem non-trivial.

In this Section, we will derive and discuss the solution and analysis of the static and dynamic problems, respectively. For brevity, the solutions given in this report are only derived using the method of dividing the core into two separate regions, which is also the most effective method (i.e. it requires the least CPU time to calculate). The derivation of the static and dynamic solutions using the method of unperturbed eigenfunctions and many more details regarding both methods are given in [4].

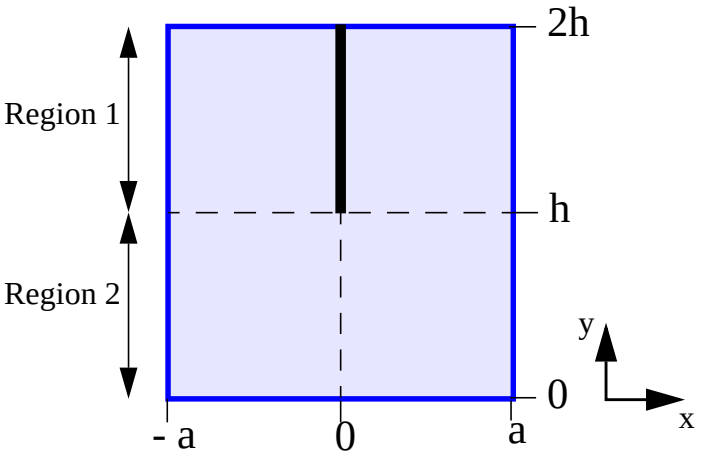

Fig. 1. The 2-D reactor model with an absorber rod present from the top to the mid-plane of the reactor.

1.2 Solution of the static problem

The model consists of a 2-D rectangular reactor of extrapolated size $2a$ by $2h$ and with an absorber rod present half-way through the reactor from the top to the mid-plane (Fig. 1). The absorber rod is the only inhomogeneity in the model and the reactor medium is otherwise considered homogeneous with constant material properties. To simplify the analytic calculations, the rod has been placed in the centre of the x-direction and in the calculations we will use one-group diffusion theory and one group of delayed neutrons. Extension to non-central rods and two-group theory is straightforward.

In this method, we divide the core into two regions: one region containing the rod $y > h$ and one without the rod $y < h$ (see Fig. 1). The result of this division is that the region for which $y > h$ will experience the presence of the absorber all through the region. Thus the x- and y-variables can be disconnected from each other and the method of separation of variables can be used for each region.

For Region 1, we have the diffusion equation

$$\Delta\phi_1(x,y) + B^2\phi_1(x,y) - \frac{\gamma}{D}\delta(x)\phi_1(x,y) = 0 \qquad (1)$$

where D is the diffusion coefficient and the buckling B is

$$B^2 = \frac{\frac{\nu\Sigma_f}{k} - \Sigma_a}{D} \tag{2}$$

where k is the eigenvalue of the system. However, for all practical purposes we will in the continuation use B as the eigenvalue of the system.

Using separation of variables, we obtain the solution as

$$\phi_1(x, y) = \sum_n A_n \sin\mu_{1,n}(a - |x|)\sin^*\lambda_{1,n}(2h - y) \tag{3}$$

Here, the functions

$$\phi_n(x) = \sin\mu_{1,n}(a - |x|) \tag{4}$$

are the solutions to the 1-D diffusion equation in Region 1, i.e.

$$\frac{d^2}{dx^2}\phi_n(x) + \mu_{1,n}^2\phi_n(x) - \frac{\gamma}{D}\delta(x)\phi_n(x) = 0 \tag{5}$$

with the boundary conditions

$$\phi_n(x) = 0 \qquad x = \pm a \tag{6}$$

The boundary conditions here are automatically fulfilled by the choice of ϕ_n in the form (4). Integration of (5) between $x = -\varepsilon$ and $x = \varepsilon$ and letting $\varepsilon \to 0$ yields the values of $\mu_{1,n}$ with which (5) is fulfilled in form of a transcendental equation

$$\mu_{1,n} = -\frac{\gamma}{2D}\tan\mu_{1,n}a \tag{7}$$

The values of $\lambda_{1,n}$ are then chosen such that each member of the sum in (3) satisfies equation (1). This is achieved by the following choice:

$$\begin{aligned} \lambda_{1,n}^2 &= B^2 - \mu_{1,n}^2 \qquad B^2 \geq \mu_{1,n}^2 \\ \lambda_{1,n}^2 &= \mu_{1,n}^2 - B^2 \qquad B^2 < \mu_{1,n}^2 \end{aligned} \tag{8}$$

and the functions $\sin^*\lambda_{1,n}(2h - y)$ are defined as

$$\sin^*\lambda_{1,n}(2h - y) = \begin{cases} \sin\lambda_{1,n}(2h - y) & B^2 \geq \mu_{1,n}^2 \\ \sinh\lambda_{1,n}(2h - y) & B^2 < \mu_{1,n}^2 \end{cases} \tag{9}$$

This way all eigenvalues $\lambda_{1,n}$ and eigenfunctions of the form (9) will be real. Formally, of course, one could use either sin or sinh functions only, with negative values of $\lambda_{1,n}^2$ and thus imaginary $\lambda_{1,n}$ for all $\lambda_{1,n}$ above certain n value. It was only for the sake of conven-

ience in the numerical evaluations that we chose the above values and conventions.

From the above it follows that each member of the sum fulfils (1) including the discontinuity of the x-derivative at $x = 0$, and the boundary conditions

$$\begin{aligned} \phi_1(\pm a, y) &= 0 \\ \phi_1(x, 2h) &= 0 \end{aligned} \tag{10}$$

The only hitherto unspecified quantities are the coefficients A_n. The coefficients will be derived from the interface condition between regions 1 and 2.

For Region 2, the diffusion equation reads

$$\Delta\phi_2(x, y) + B^2\phi_2(x, y) = 0 \tag{11}$$

The boundary conditions for this region are

$$\begin{aligned} \phi_2(\pm a, y) &= 0 \\ \phi_2(x, 0) &= 0 \end{aligned} \tag{12}$$

The solution from separation of variables becomes

$$\phi_2(x, y) = \sum_{n=1}^{N} C_n \cos\mu_{2,n} x \sin^*\lambda_{2,n} y \tag{13}$$

where

$$\mu_{2,n} = \frac{2n-1}{2a}\pi \qquad n = 1, \ldots, \mathrm{N}. \tag{14}$$

Further, $\lambda_{2,n}$ and $\sin^*\lambda_{2,n} y$ are defined similarly as (8) and (9), respectively.

The continuity conditions at the interface between the two regions are

$$\phi_1(x, h) = \phi_2(x, h) \tag{15}$$

and

$$\left.\frac{\partial}{\partial y}\phi_1(x, y)\right|_{y=h} = \left.\frac{\partial}{\partial y}\phi_2(x, y)\right|_{y=h} \tag{16}$$

where we have used the fact that the diffusion coefficients are equal for the two regions. Inserting (3) and (13) into (15) and (16), multiplying with $\cos\mu_{2,p} x$ and integrating, we obtain the two equations

$$C_p = \sum_n A_n \frac{\sin^* \lambda_{1,n} h}{\sin^* \lambda_{2,p} h} \cdot \frac{1}{a} \int_{-a}^{a} \sin \mu_{1,n} (a - |x|) \cos \mu_{2,p} x dx \tag{17}$$

and

$$C_p = -\sum_n A_n \frac{\lambda_{1,n} \cos^* \lambda_{1,n} h}{\lambda_{2,p} \cos^* \lambda_{2,p} h} \cdot \frac{1}{a} \int_{-a}^{a} \sin \mu_{1,n} (a - |x|) \cos \mu_{2,p} x dx \tag{18}$$

Both equations above can now simply be written in matrix form as

$$\boldsymbol{c} = \boldsymbol{M}\boldsymbol{a} \tag{19}$$

and

$$\boldsymbol{c} = \boldsymbol{K}\boldsymbol{a} \tag{20}$$

where the column vectors $\boldsymbol{a}$ and $\boldsymbol{c}$ contain the coefficients A_n and C_p as their elements, respectively. The elements of the matrices $\boldsymbol{M}$ and $\boldsymbol{K}$ are defined through (17) and (18).

By taking the difference between equations (19) and (20) above, we obtain the eigenvalue equation for the flux as

$$(\boldsymbol{M} - \boldsymbol{L})\boldsymbol{a} = \boldsymbol{0} \tag{21}$$

and the criticality equation becomes

$$det(\boldsymbol{M} - \boldsymbol{L}) = 0 \tag{22}$$

From (21), both the fundamental and symmetric higher order eigenmodes can be calculated.

The static flux has been calculated from (21) and the result is given in Fig. 2 together with the critical buckling B. The reactivity value of the rod in Fig. 2 is -0.41 $ or -310 pcm. We have intentionally selected a strong rod to illustrate the resulting depression of the flux around the absorber. The flux gradient w.r.t. the x-direction is discontinuous across the absorber as it should. The rod also forces the axial maximum of the flux downward, below the geometrical centre of the reactor. It is further interesting to note how the effect of the rod vanishes close to the rod edge.

In the neighbourhood of the rod edge, the flux is rather strongly distorted and this can be applied to the identification of the axial position of the rod tip [11], [12]. The neutron current, or the gradient of the flux assuming diffusion theory, is even more sensitive to the position of the rod edge. The present model has already been used to illustrate the possible applications of the neutron current in core monitoring and diagnostics [10].

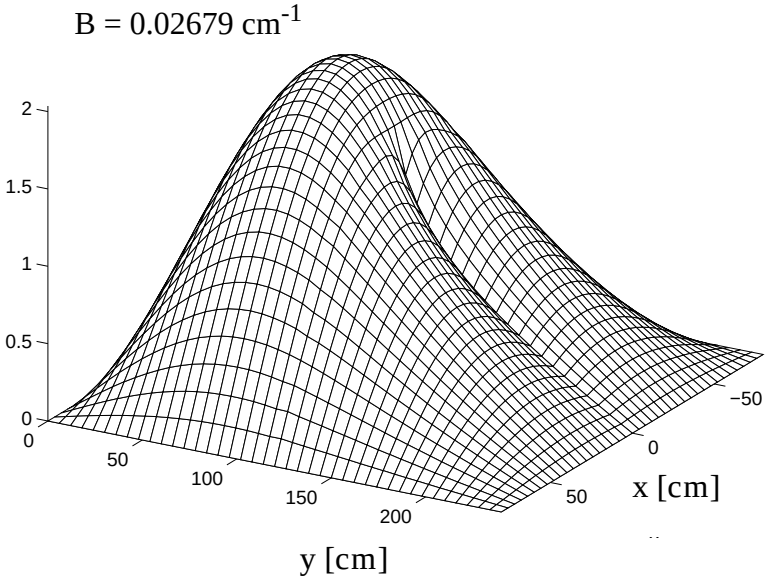

Fig. 2. The static neutron flux. Notice the depression of the flux caused by the presence of the absorber rod and also that the flux maximum is pushed down from the centre of the reactor.

1.3 Solution of the dynamic (noise) problem

We will now apply the methods described in the previous section to find the exact solution to the noise due to vertical oscillations (vibration) of an absorber rod in a 2-D system. The vertical oscillations of the rod can be described by the time-dependent macroscopic absorption cross-section as

$$\Sigma_a^r(x, y, t) = \gamma\delta(x)\Theta(y - h - \varepsilon(t)) \tag{23}$$

where $\varepsilon(t)$ is the vibration amplitude in the positive y-direction. By expanding (23) in a Taylor series around $\varepsilon(t) = 0$ and neglecting second and higher order terms in ε, we obtain the perturbation represented by the oscillations as

$$\delta\Sigma_a(x, y, t) = -\varepsilon(t)\gamma\delta(x)\delta(y - h) \tag{24}$$

This corresponds to a point source of variable strength, positioned at the tip of the rod.

By introducing the time-dependent absorption cross-section into the time-dependent one-group diffusion equation with one-group of delayed neutrons, linearizing and making a Fourier transformation, the resulting noise equation is obtained as

$$\Delta\delta\phi(x, y, \omega) + B^2(\omega)\delta\phi(x, y, \omega) - \frac{\gamma}{D}\delta(x)\Theta(y - h)\delta\phi(x, y, \omega) = S(x, y, \omega) \tag{25}$$

where

$$B^2(\omega) = B_0^2\left(1 - \frac{1}{\rho_\infty G_0(\omega)}\right) \tag{26}$$

and

$$S(x, y, \omega) = \frac{\delta\Sigma_a(x, y, \omega)\phi(x, y)}{D} = -\varepsilon(t)\frac{\gamma}{D}\delta(x)\delta(y - h)\phi(x, y) \tag{27}$$

The static flux which is present in the noise source (27) acts as a scaling factor for the source amplitude. The boundary conditions for the noise equation are the same as those for the static equation.

The equation for the noise (25) is now complex due to the presence of the complex zero reactor transfer function $G_0(\omega)$ in (26) and thus we expect the equation to have a complex solution. Therefore, we have chosen to numerically determine the solution using fully complex quantities in the continuation.

The exact solution for the noise can be obtained using the method of dividing the reactor into two regions. Assume first that the noise can be expanded similarly as in the static case. We can write the noise as

$$\delta\phi_1(x, y, \omega) = \sum_{n=1}^{N} A_n(\omega)\sin\mu_{1,n}(a - |x|)\sin\lambda_{1,n}(2h - y) \tag{28}$$

for Region 1 and similarly for Region 2, we have

$$\delta\phi_2(x, y, \omega) = \sum_{n=1}^{N} C_n(\omega)\cos\mu_{2,n}x\sin\lambda_{2,n}y \tag{29}$$

The effect of the noise source is taken into account by modifying the current continuity interface condition in (16). The modified interface condition is obtained in the same way as we took the absorber rod into account in the solution for the static flux in region one. Thus, we integrate the noise equation (25) between $y = h - \varepsilon$ and $y = h + \varepsilon$ and let ε tend to zero. This yields the modified continuity condition for the current (i.e. the gradient of the flux) as

$$\frac{\partial}{\partial y}\delta\phi_1(x, y, \omega)\Big|_{y=h} - \frac{\partial}{\partial y}\delta\phi_2(x, y, \omega)\Big|_{y=h} = -\varepsilon(\omega)\frac{\gamma}{D}\delta(x)\phi(x, h) \tag{30}$$

The continuity condition for the flux is the same as in equation (15).

Putting (29) into (30) and (15), multiplying with $\cos\mu_{2,p}x$ and integrating, we obtain the following expressions

$$\sum_n A_n \frac{\lambda_{1,n}\cos\lambda_{1,n}h}{\lambda_{2,p}\cos\lambda_{2,p}h}\cdot\frac{1}{a}\int_{-a}^{a}\sin\mu_{1,n}(a-|x|)\cos\mu_{2,p}x\,dx + C_p = \\ = \varepsilon(\omega)\frac{\gamma}{Da}\phi(0,h)\cdot\frac{1}{\lambda_{2,p}\cos\lambda_{2,p}h} \tag{31}$$

and

$$C_p = \sum_n A_n \frac{\sin\lambda_{1,n}h}{\sin\lambda_{2,p}h}\cdot\frac{1}{a}\int_{-a}^{a}\sin\mu_{1,n}(a-|x|)\cos\mu_{2,p}x\,dx \tag{32}$$

We can write the equations in matrix form as

$$\boldsymbol{R}\boldsymbol{a} + \boldsymbol{c} = \boldsymbol{d} \tag{33}$$

and

$$\boldsymbol{c} = \boldsymbol{P}\boldsymbol{a} \tag{34}$$

As expected, due to the inhomogeneous term $\boldsymbol{d}$ in (33), corresponding to the r.h.s. of (31), these equations are not eigenvalue equations. The coefficient vectors $\boldsymbol{a}$ and $\boldsymbol{c}$ can be calculated by rearrangement as

$$\boldsymbol{a} = (\boldsymbol{R}+\boldsymbol{P})^{-1}\boldsymbol{d} \\ \boldsymbol{c} = \boldsymbol{P}\boldsymbol{a} \tag{35}$$

The neutron noise is obtained by calculating the coefficient vectors $\boldsymbol{a}$ and $\boldsymbol{c}$ from (35) and then using them in the expressions for the noise (28) and (29).

The amplitude and phase of the induced noise resulting from axial oscillations of 1 cm amplitude of the absorber rod is shown in Figs. 3 and 4, respectively, for a few selected frequencies. At low frequencies, the noise behaves in a point kinetic fashion, with a phase that is constant in space and an amplitude which has the same space-dependence as the static flux. With increasing frequencies, both the amplitude and the phase delay become more and more space dependent, the fastest changes being concentrated around the perturbation (source).

1.4 Conclusions

Because of the straightforward manner in which both the static and the dynamic problem can be solved in this model, it is also suitable for analytical and numerical studies of the applicability of various reactor kinetic approximations (point kinetic, adiabatic, prompt jump approximations). It also constitutes a fairly realistic and powerful description of realistic cases, i.e. partially inserted control rod and the so-called rod manoeuvring experiment. It is going to be used for comparison with calculations from ICFM codes [6] as well as with eventual later experiments. Finally, the work has also some pedagogical value in nuclear engineering education, giving an advanced example of the separation of variables.

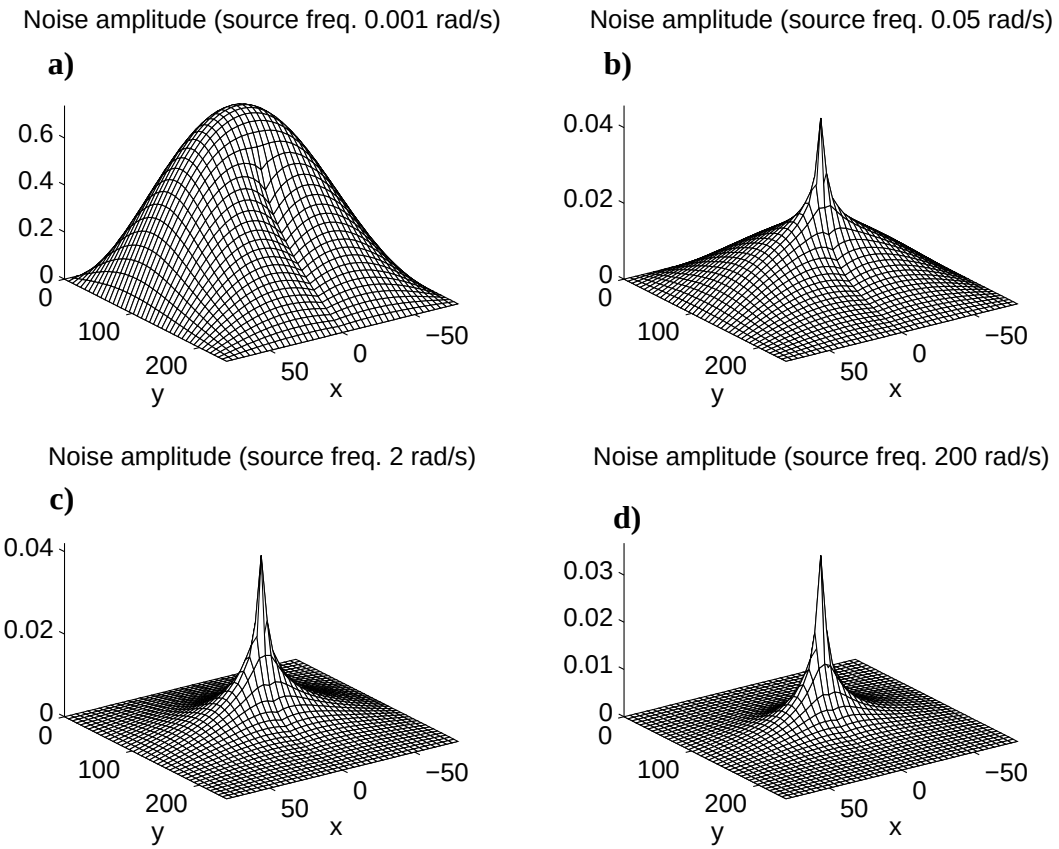

Fig. 3. The amplitude of the noise for four different frequencies of the source oscillation.

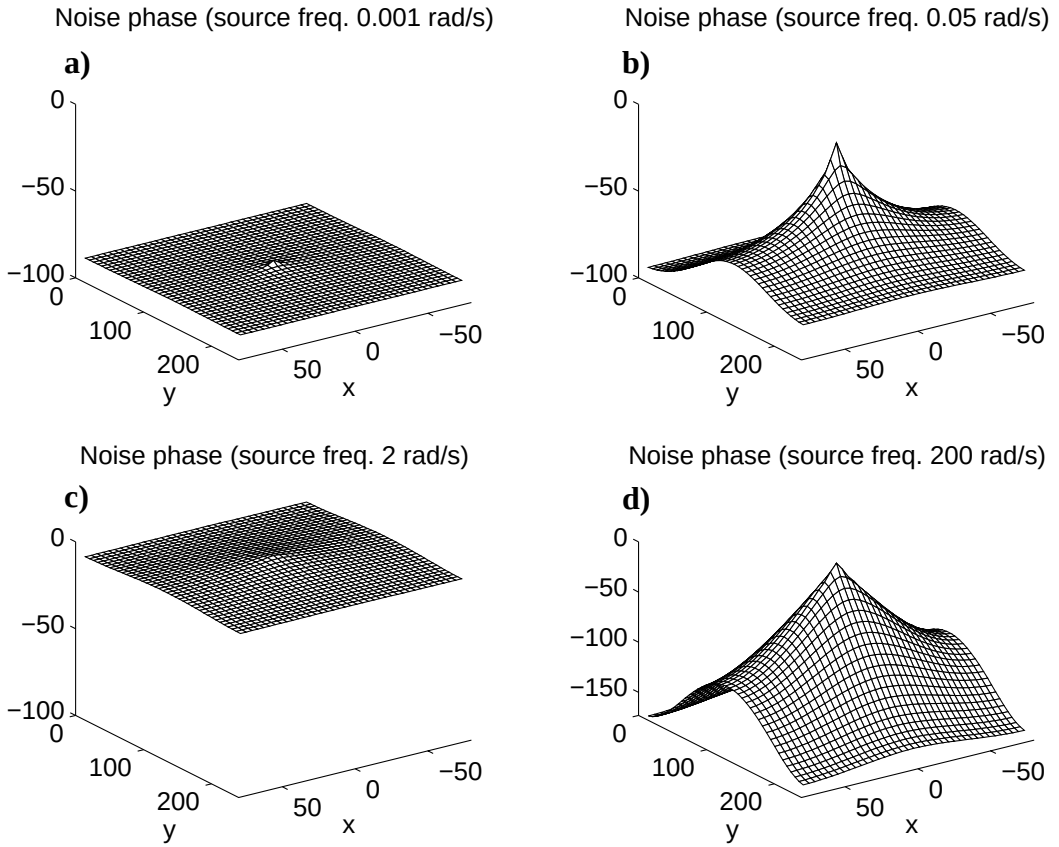

Fig. 4. The phase of the noise for four different frequencies of the source oscillation.

Section 2

Evaluation of the adiabatic approximation in the reactor model described in the previous Section

2.1 General

In many problems of reactor noise diagnostics, it may be of significant advantage to solve the time- or frequency dependent equations for the neutron noise in some reactor physics approximation. The simplest non-trivial approximation is the adiabatic approximation, which was already described in the previous Stage (Ref. [3]). The advantages of its use are twofold. First, the solution via the adiabatic approximation lends itself to a simple physical interpretation, which enhances the understanding and interpretation of various phenomena. This may have the further advantage that it even may help to elaborate unfolding (inversion) methods for diagnostical problems. Second, mathematically it is simpler than the exact method. In particular, at present the adiabatic approximation is the only one that can be used to estimate the neutron noise in real (inhomogeneous) reactor cores, by using existing ICFM codes.

This latter principle was demonstrated in the previous Stage where the neutron noise induced by a rod manoeuvring experiment was calculated by using SIMULATE together with the adiabatic approximation ("SIMULATE-Adiabatic", see Ref. [3]). However, one problem with the above mentioned procedure was that in absence of an "exact" solution, it was not possible to estimate the precision of the SIMULATE-Adiabatic algorithm.

The axially non-homogeneous reactor model, described in the previous Section, gives a possibility to assess the suitability of SIMULATE-Adiabatic. Namely, in this model, both the exact and the adiabatic solutions can be obtained to the same perturbation, in a non-trivial model that is sufficiently similar to the SIMULATE calculations. Thus, some indications of the suitability of SIMULATE-Adiabatic can be obtained. This is the purpose of the present Section.

2.2 The adiabatic approximation

The concept of the adiabatic approximation and its application to the rod manoeuvring experiment were described in Stage 3 (Ref [3]), thus they will only be described very briefly here. The essence is to factorize the time-dependent flux into an amplitude and a shape function as

$$\phi(x, y, t) = P(t)\Psi(x, y, t) \tag{36}$$

with the normalizing condition for the shape function in the form

$$\int_{-a}^{a}\int_{0}^{2h} \phi_0(x,y)\Psi(x,y,t)dydx \;=\; \int_{-a}^{a}\int_{0}^{2h} \phi_0^2(x,y)dydx \tag{37}$$

where $\phi_0(x,y)$ is the static flux. The above formulae are written directly in a 2-D x-y geometry, such that they suit the 2-D model of the previous Section.

Expressions for the neutron noise can be obtained from (36) by splitting all components into a sum of a steady-state (time-independent) component and time- (frequency-) dependent fluctuations as

$$\phi(x,y,t) \;=\; \phi_0(x,y) + \delta\phi(x,y,t) \tag{38}$$

$$P(t) \;=\; 1 + \delta P(t) \tag{39}$$

$$\Psi(x,y,t) \;=\; \phi_0(x,y) + \delta\Psi(x,y,t) \tag{40}$$

With (38) - (40), and assuming small fluctuations (neglecting second order terms), the noise can be expressed as

$$\delta\phi(x,y,t) \;=\; \delta P(t)\phi_0(x,y) + \delta\Psi(x,y,t) \tag{41}$$

The first term on the r.h.s. is called the reactivity or point kinetics component, and the second the space dependent component. Due to the linearisation process, this term is independent of whether or not a reactor kinetic approximation is used. As is well known, this term is given as the solution of the linearized point kinetics equations, whose solution in the frequency domain is given as

$$\delta P(\omega) \;=\; G_0(\omega)\cdot\rho(\omega) \tag{42}$$

where $G_0(\omega)$ is the zero reactor transfer function. Again, due to linearity, the reactivity can be calculated from a perturbation formula involving only the static flux and the perturbation in the cross sections.

Application of the adiabatic approximation affects only the second term. It means that the space-dependent term $\delta\Psi(x,y,t)$ is determined from a static calculation. In other words, $\delta\Psi(x,y,t)$ is calculated as the difference between two static fluxes, one belonging to the critical (reference) state, the other is the flux from a criticality (eigenvalue) calculation belonging to the perturbed reactor at time *t*.

Concretely, in our case, the critical equation is given as

$$\Delta\phi_0(x,y) + B^2\phi_0(x,y) - \frac{\gamma}{D}\delta(x)\Theta(y-h)\phi_0(x,y) \;=\; 0 \tag{43}$$

and the static eigenvalue equation with the rod withdrawn from the critical position with a distance $\varepsilon(t)$ is

$$\Delta\Psi_{ad}(x, y, t) + B_p^2\Psi_{ad}(x, y, t) - \frac{\gamma}{D}\delta(x)\Theta(y - [h + \varepsilon(t)])\Psi_{ad}(x, y, t) = 0 \qquad (44)$$

where the eigenvalue of the perturbed state is contained in the perturbed buckling B_p^2. From here the adiabatic approximation of $\delta\Psi(x, y, t)$ is given as

$$\delta\Psi_{ad}(x, y, t) = \Psi_{ad}(x, y, t) - \phi_0(x, y) \qquad (45)$$

Naturally, in order to obtain correct results, $\Psi_{ad}(x, y, t)$ and $\phi_0(x, y)$ need to be normalized in a proper way, i.e. $\Psi_{ad}(x, y, t)$ must satisfy (37).

Collecting both components of the noise, the final form of the adiabatic approximation of the neutron noise in the frequency domain can be written as

$$\delta\phi_{ad}(x, y, \omega) = G_0(\omega)\rho(\omega)\phi_0(x, y) + \delta\Psi_{ad}(x, y, \omega) \qquad (46)$$

Again, because of linearity, i.e. neglection of higher order terms in the perturbation, both terms on the r.h.s. will be linear in the perturbation parameter, in our case $\varepsilon(\omega)$. This is because for small movements of the rod, the perturbation of the absorption cross section $\Sigma_a(x, y, t)$ can be represented as

$$\begin{aligned}\Sigma_a(x, y, t) &= \frac{\gamma}{D}\{\delta(x)\Theta(y - [h + \varepsilon(t)]) - \delta(x)\Theta(y - h)\} \\ &\sim -\frac{\gamma}{D}\varepsilon(t)\delta(x)\delta(y - h)\end{aligned} \qquad (47)$$

Thus the perturbation is equivalent to a time-varying point source of a time-dependent strength equal to $\varepsilon(t)$. As a consequence, both the reactivity term and the space-dependent term will be linear in $\varepsilon(t)$ ($\varepsilon(\omega)$). The system response can then be characterised by

$$\frac{\delta\phi_{ad}(x, y, \omega)}{\varepsilon(\omega)} \qquad (48)$$

It is this quantity which will be shown in the quantitative work below. From the above it also follows that both ρ/ε and $\delta\Psi_{ad}/\varepsilon$ are independent of the frequency of the perturbation. The only frequency dependence in (48) arises from the zero reactor transfer function, $G_0(\omega)$.

2.3 Quantitative results

A quantitative analysis of the adiabatic approximation, applied to the rod manoeuvring experiment, was performed in the same reactor model as in the previous Section. A summary of the results is shown in Figs. 5 and 6. In both figures, the space dependence of the noise along a horizontal cross section of the core, i.e. along the x-axis, is shown at several axial elevations (y-values). In all figures the exact solution, the point kinetic component and the noise in the adiabatic approximation is shown.

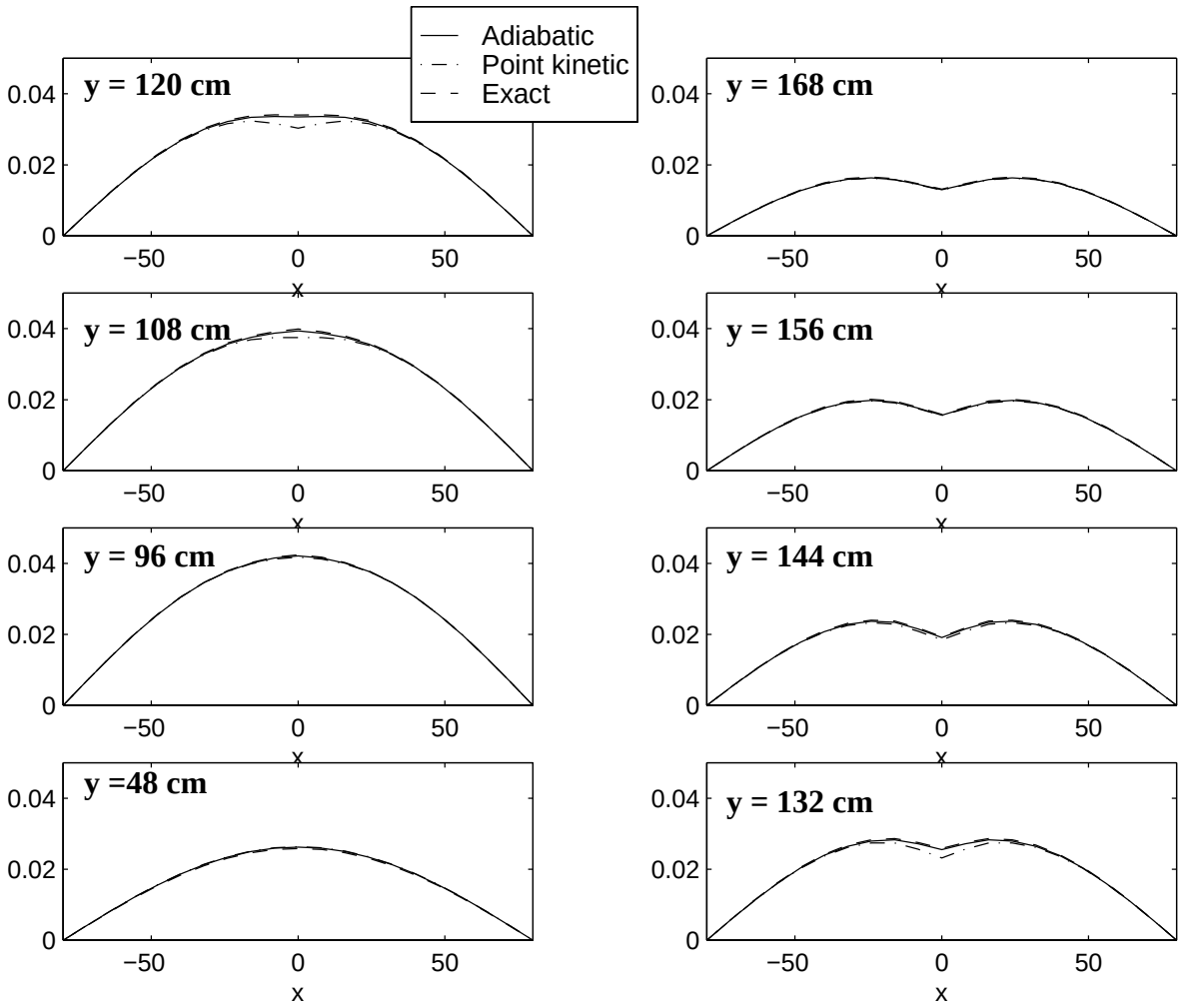

Fig. 5. The space dependence of the neutron noise along the x-axis at several axial elevations at ω *=0.01 rad/s. The rod tip (perturbation position) is located at y=120 cm.*

At the lower frequency of ω = 0.01 rad/sec (Fig. 5), the system response is rather point kinetic. All three solutions (point kinetic, adiabatic, exact) are very close to each other, and the space dependence of the noise is equal to that of the static flux. This agrees with the SIMULATE-Adiabatic results in [3], Fig. 16, except that a deviation was found there between the adiabatic and point kinetic terms in the close vicinity of the rod tip (perturbation point) which is absent in the results of the present analysis. The reason for this difference is that this deviation is due to the local component of the noise, which can only be accounted for in 2-group theory. SIMULATE can thus reconstruct this local term, but our present 1-group model cannot.

At the higher frequency of ω=0.1 rad/sec, the deviations from point kinetic behaviour are significantly larger, especially close to the perturbation point (Fig. 6.). At the same time, the adiabatic approximation is still quite close to the exact solution, indicating that this approximation is quite good at this reactor size and perturbation frequency. Also, these results are in a quite good qualitative agreement with the SIMULATE-Adiabatic calcula-

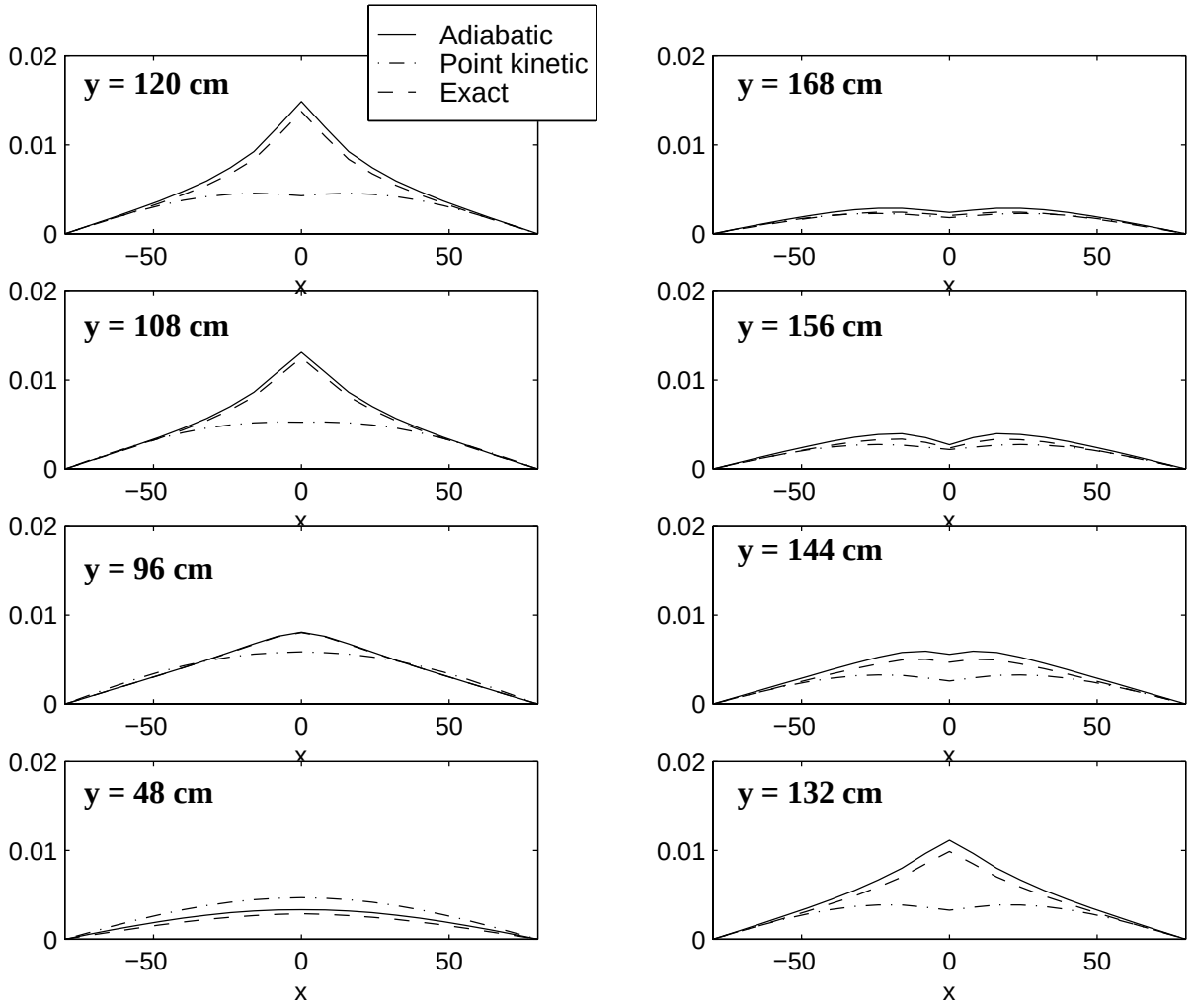

Fig. 6. The space dependence of the neutron noise along the x-axis at several axial elevations at ω =0.1 rad/s. The rod tip (perturbation position) is located at y=120 cm.

tions, Ref. [3], Figs. 17 and 18. The differences between these and the results in Fig. 6 here are much smaller than in the previous case of low frequency, mainly because of the fact that the local component plays a much smaller role in this case (due to the overall strong space dependence of the noise).

It is thus concluded that the above analysis confirms our previous expectation that the method SIMULATE-Adiabatic can be a useful tool to calculate the neutronic response to certain perturbations. Of course the method is applicable within a limited frequency range only, and in each application a separate judgement need to be made to confirm the applicability. However, since at present there are no dynamic codes available to calculate the space-dependent neutron noise in real heterogeneous reactors, it is very useful to have access to such adiabatic methods that can be used with existing codes.

The above figures show only the noise along certain cross sections of the core in a one-dimensional manner. It may be of interest to see the noise in the whole 2-D region of the reactor. In Fig. 7a the space dependent component in the adiabatic approximation,

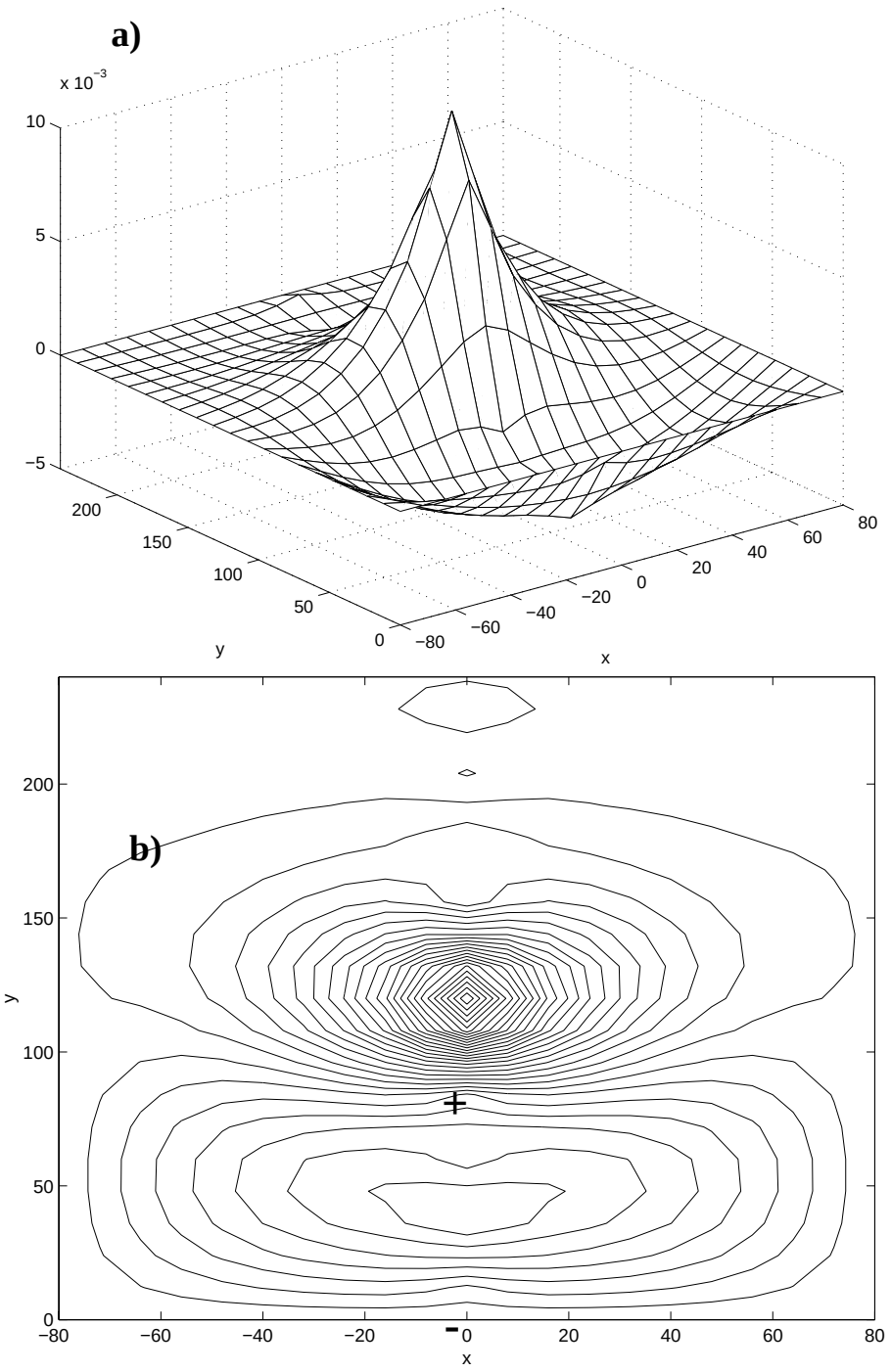

Fig. 7. The space dependence of the space-dependent component of the noise in the adiabatic approximation: a) 2-D plot; b) contour plot, showing the areas of positive and negative values.

$\delta\Psi_{ad}(x, y, \omega)/\varepsilon(\omega)$, is shown as a 2-D function. Due to the normalisation condition (37), $\delta\Psi_{ad}$ is orthogonal to the static flux, and thus it must have both positive and negative values. The areas of positive and negative values are clearly seen in the figure, especially on the contour plot (Fig. 7b).

A more detailed report on the above results will be published separately (Ref. [5]).

Section 3

Development of methods for the separation of concurrent global and regional power oscillations in boiling water reactors (BWRs)

3.1 Introduction

Stability measurements performed in Ringhals 1 during start-up 1990 showed that limit cycle power oscillations occurred at 72.6% power and a core flow of 3694 kg/s. Analysis of the phase relationships between the different local power range monitors (LPRMs) showed that the first azimuthal mode was responsible for the oscillations (out-of-phase oscillations). Measurements performed in a nearby point on the power-flow map indicated a stable situation with a DR of approximately 0.7. Further, the phase between LPRMs in this operating point showed that the power oscillations were in-phase.

The oscillations in both operating points occurred at the same frequency. This may seem like a contradiction, but in fact the explanation is that an in-phase (global) mode was present simultaneously with an out-of-phase (regional) mode and at the same frequency. These two modes had different amplitudes and different stability properties. The amplitude of the two modes depended strongly on the operating point, with the effect that a change of operating point seemed to make the DR "jump" from a value of ~0.7 directly to unity. It was then realised, that in this case the conventional DR did not give an appropriate indication of how close one was to instability. In order to resolve this problem, the two flux modes need to be separated and their DRs determined independently.

The out-of-phase component can be obtained by taking a weighted difference of signals from detectors 180° diagonally separated in the reactor. This method, which is called the subtraction method, relies on the symmetry of the out-of-phase mode and the result is that in-phase components common to both detector signals cancel, while out-of-phase components are somewhat enhanced. A similar procedure was used with success to determine the stability properties of the global and regional modes in the Ringhals case [7]. This method has also become the most widely used procedure so far in separation of global and out-of-phase modes in BWRs.

Alternatively, a decomposition method based on the factorisation of the flux can be used to obtain the modes separately. This so called factorisation method, described more in detail below, has been attempted already in Ref. [7], but without success. The work described here started with the purpose of understanding the reason of the failure.

To summarize the results, the explanation of the failure lies in two facts. One is the approximate character of the factorization formula, approximating an integral over the core with a discrete sum over a number of detectors. The second is the presence of the local component of the noise (generation and axial propagation of the void), which introduces strong correlations between detectors in the same axial string. These two facts together introduce

extra components into the correlation functions from which the decay ratio is determined, hence leading to incorrect estimate of the decay ratio.

The work presented in this Section gives a quantitative description of the above facts. Based on the analysis, it was also found that a factorisation technique that is based on detector signals from one axial level only, gives very good results. We call this method the "partial factorisation technique". Its use will be also demonstrated through an analysis of the Ringhals measurements.

The work described here has been accepted for publication in *Nucl. Sci. Engng.* [9]. The current chapter summarizes the main findings, though a more detailed account of the work performed is given in [9].

3.2 The factorisation method

The space-time dependent flux can be factorised into an amplitude and a shape function as

$$\phi(\boldsymbol{r}, t) = P(t)\Psi(\boldsymbol{r}, t) \tag{49}$$

Assuming that the time-dependent fluctuations of the quantities in (49) are all small, each of them can be written as composed of a sum of a steady state value and a small time-dependent perturbation. These expressions can be substituted into (49) and, after some simplification, we obtain

$$\delta\phi(\boldsymbol{r}, t) = \delta P(t)\phi_0(\boldsymbol{r}) + \delta\Psi(\boldsymbol{r}, t) \tag{50}$$

The first term in (50) represents the fluctuations of the global mode (i.e. it has the same spatial dependence as the static flux $\phi_0(\boldsymbol{r})$). The second term $\delta\Psi(\boldsymbol{r}, t)$ in (50) contains all other fluctuations (i.e. higher order modes as well as a local component of the noise) present in the reactor. This term will be called the space-dependent component.

For (50) to be unambiguous it is sufficient to require that:

$$\int_V \phi_0(\boldsymbol{r})\delta\Psi(\boldsymbol{r}, t)dV = 0 \tag{51}$$

This integral expresses the fact that the shape function $\delta\Psi$ must be orthogonal to the static flux. Thus by multiplying (50) with the static flux $\phi_0(\boldsymbol{r})$ and integrating over the core volume, the time-dependence of the reactivity component can be obtained as

$$\delta P(t) = \frac{\int_V \phi_0(\boldsymbol{r})\delta\phi(\boldsymbol{r}, t)dV}{\int_V \phi_0^2(\boldsymbol{r})dV} \approx \frac{\sum_{i=1}^{M} \phi_0(\boldsymbol{r}_i)\delta\phi(\boldsymbol{r}_i, t)}{\sum_{i=1}^{M} \phi_0^2(\boldsymbol{r}_i)} \tag{52}$$

where the r.h.s was obtained by approximating the integrals with sums over a number of detectors M. Here, the static flux $\phi_0(\boldsymbol{r}_i)$ and the noise signal $\delta\phi(\boldsymbol{r}_i, t)$ are obtained from the mean value and fluctuating part of the detector signal i, respectively. The space-dependent, i.e. non-global part, of the signals can now be calculated using (50) as

$$\delta\Psi(\boldsymbol{r}, t) = \delta\phi(\boldsymbol{r}, t) - \delta P(t)\phi_0(\boldsymbol{r}) \tag{53}$$

Assuming now that the space-dependent component consists only of the first azimuthal mode, i.e. $\delta\Psi(\boldsymbol{r}, t) = \delta R(t)\phi_1(\boldsymbol{r})$, this method should be able to separate the two modes present in the Ringhals measurements. This separation procedure was also attempted in [7], where it was called the global/space dependent separation method, but without success.

No logical explanation of this failure was found at the time the original analysis was performed, especially not in the light of the successful separation obtained by using the subtraction method on the same data. One would actually expect the factorisation method to be more accurate in practice, since it has several inherent advantages that should counteract the deleterious effects of the applied approximations. The advantages of the factorisation method are the use of a large number of detectors in (52) and that the static flux is obtained from the measurement itself.

However, at one stage we realised that quite plausible results could be obtained with the factorisation based technique, if the orthogonality integral was approximated by a sum over 36 detectors of one axial level, instead of all 72 detectors that are situated on two different axial levels. The reason for the success of the factorisation method when detectors on a single axial level are used, compared to its failure when all detectors are used, lies in the presence of local noise fluctuations in the space-dependent component $\delta\Psi$ in addition to the mode oscillations. This statement will be confirmed in the next subsection via a simple phenomenological model of BWR noise. The factorisation method using detectors from a single axial level only will be called the partial factorisation method in the continuation.

3.3 A phenomenological model of BWR noise

The success of the partial factorisation procedure may be understood through the use of a phenomenological model of BWR noise. This model of the noise must contain both global oscillations $(\delta P(t)\phi_0(\boldsymbol{r}))$ and out-of-phase ones $(\delta R(t)\phi_1(\boldsymbol{r}))$ as well as an (axially propagating) local component $\delta L(\boldsymbol{r}, t)$. In formulae, the noise in this model can be expressed as

$$\delta\phi(\boldsymbol{r}, t) = \delta P(t)\phi_0(\boldsymbol{r}) + \delta R(t)\phi_1(\boldsymbol{r}) + \delta L(\boldsymbol{r}, t) \tag{54}$$

In this context, the space-dependent term $\delta\Psi(\boldsymbol{r}, t)$ of (50) can now be identified as being equal to

$$\delta\Psi(\boldsymbol{r}, t) = \delta R(t)\phi_1(\boldsymbol{r}) + \delta L(\boldsymbol{r}, t) \tag{55}$$

A phenomenological model similar to (54), but without the regional mode, has been suc-

cessfully used in the past to support the analysis of BWR noise measurements.

Assuming statistical independence between the components of (54) and taking the auto-correlation of (55), we obtain

$$ACF_{\delta\Psi}(\boldsymbol{r}, \tau) = ACF_{\delta R}(\tau) \cdot \phi_1(\boldsymbol{r}) + ACF_{\delta L}(\boldsymbol{r}, \tau) \tag{56}$$

or, alternatively,

$$APSD_{\delta\Psi}(\boldsymbol{r}, \omega) = APSD_{\delta R}(\omega) \cdot \phi_1(\boldsymbol{r}) + APSD_{\delta L}(\boldsymbol{r}, \omega) \tag{57}$$

The physical properties described by the local component of the noise consist of the local void formation everywhere in the reactor and the axial upward propagation of these void fluctuations. Thus, the correlation function $ACF_{\delta L}$ of the local component has a peak centred at $\tau = 0$ with a width depending on the bandwidth of the noise. The local thermohydraulical properties that determine void formation and propagation properties, can be assumed statistically independent and thus no correlation exists between detectors at different radial positions on the same axial level. Further, if one takes the cross-correlation function between two detectors in the same string (i.e. one detector is situated directly above the other), the axial transport of the void fluctuations causes a peak to appear at $\tau = \tau_0$, where τ_0 is the transport or delay time between the two detectors. The transport time may be used to obtain the average steam velocity between the detectors. In the frequency domain, this corresponds to a linear behaviour of the phase with frequency.

The out-of-phase oscillation, on the other hand, shows a very different behaviour in its auto correlation $ACF_{\delta R}(\tau)$ and power spectrum $APSD_{\delta R}(\omega)$. Since the regional mode is best described by a damped oscillator excited by white noise, its $ACF_{\delta R}(\tau)$ will show successive damped oscillations. In the corresponding power spectrum, the oscillation yields a peak at the frequency of oscillation.

Since a small radial variation in the steam velocity exists also on a single axial level, variations will occur also in the width of the peak present in the $ACF_{\delta L}$. This can cause uncertainties in the determination of the DR for the regional component from $ACF_{\delta\Psi}$. It is thus possible to explain, only by accounting for the local component, why the space-dependent component deviates from the out-of-phase mode, and in particular, why the decay ratio derived from $\delta\Psi$ remains space dependent. However, since the axial variation is considerably greater, one notes that some differences may be expected whether detectors from one elevation or two elevations are used in the approximate factorisation method, respectively.

This explains the appearance of space-dependent DRs, but the approximations made in the summation step (52) need also to be taken into account for a full explanation. Details of this analysis are given in [9], here we only summarize the findings. By taking into account the approximations performed and by using detector signals from one axial level only, the result for the auto-correlation function of the space-dependent component $\delta\Psi_{appr}$ is obtained as

$$ACF_{\delta\Psi_{appr}}(\boldsymbol{r}_i, \tau) = A_1^2\phi_1^2(\boldsymbol{r}_i)ACF_{\delta R}(\tau) + A_2^2 ACF_{\delta L}(\boldsymbol{r}_i, \tau) + \varepsilon_i{}^2\phi_0^2(\boldsymbol{r}_i)ACF_{\delta P}(\tau) \quad (58)$$

where $A_1 \cong 1$, $A_2 \cong 1$ and $\varepsilon_i{}^2 \ll 1$.

Equation (58) shows a structure similar to (56), but a difference is the presence of the ACF of the global component in (58), although with a small weight. The presence of the local and global components in the space-dependent signal $\delta\Psi_{appr}(\boldsymbol{r}, t)$ causes the decay ratio, derived from $\delta\Psi_{appr}(\boldsymbol{r}, t)$ to deviate from that of the desired out-of-phase component. The same is true for the global component $\delta P_{appr}(t)$. Due to the axial dependence of $ACF_{\delta L}(\boldsymbol{r}, \tau)$, even in this case it is obvious that the decay ratios, either global or out-of-phase, will be axially dependent. However, with a relatively large number of detectors this dependence will be weak, and a rather good approximation of the global and out-of-phase decay ratios should be obtained.

We will now contrast the above results with those obtained in case the detectors used in the summation are situated at two different axial levels. This corresponds to the factorisation method as it was employed in [7]. The resulting ACF for this case is

$$\begin{aligned} ACF_{\delta\Psi_{appr}}(\boldsymbol{r}_i, \tau) &= A_1^2\phi_1^2(\boldsymbol{r}_i)ACF_{\delta R}(\tau) + A_2^2 ACF_{\delta L}(\boldsymbol{r}_i, \tau) + \\ &+ \varepsilon_1^2\phi_0^2(\boldsymbol{r}_i)ACF_{\delta P}(\tau) + \varepsilon_{ii'}CCF_{\delta L}(\boldsymbol{r}_i, \boldsymbol{r}_i', \tau) + \varepsilon_2^2\overline{CCF_{\delta L}(\tau)} \end{aligned} \quad (59)$$

Here, the summation extends over all 72 detectors corresponding to the Ringhals measurements. The primes are used to distinguish between the lower and upper axial position. Thus $\boldsymbol{r}_i$ and $\boldsymbol{r}_i'$ are the two detector positions within the same detector string.

Equation (59) contains the same terms as (58), but in addition it also contains the cross-correlations of the local noise between detectors in the same string, c.f. the last two terms of the equation. These additional cross-correlation terms influence the determination of a DR from (59) in a different and more important way than the preceding ones. The difference is that the cross correlations $CCF_{\delta L}(\boldsymbol{r}_j, \boldsymbol{r}_j', \tau)$ have a peak at a value $\tau_0 > 0$ where τ_0 is the transport time of the void fluctuations between the two axial levels. In addition, since this transport time may vary substantially between the different radial positions, $CCF_{\delta L}(\tau)$ may show a much broader peak than the individual CCFs. The weight of the second last term in (59) is also larger than that of the last term in (58).

It is thus seen that there is a significant difference regarding whether detectors from one level only or detectors from two (or more) levels are used. Reasonably good results can be obtained for the global and regional decay ratios if detectors from one level are used. If detectors from at least two levels are used in the flux decomposition procedure, then reconstruction of the in-phase and out-of-phase components is practically not possible. This is why the attempt made in [7] was not successful. Not only become the ACFs of the global and out-of-phase components "distorted" by the presence of the cross-correlation of the local term, but this latter term also distorts the phase relationships of the factorised signals $\delta\Psi(\boldsymbol{r}_i, t)$, such that the out-of-phase quality of the signal is perturbed.

Because of these difficulties, the method of subtraction is both simpler and more effective. It is also possible to explain why it worked better in [7] than the factorisation method. The reason is that in the subtraction method detectors from the same axial level were used, whereas in the factorisation method, from both axial elevations. However, it is also seen that the problems of factorisation can be avoid if only detectors from one axial level are used. This so-called partial factorisation technique was suggested to use and tested in some detail in this work.

3.4 Application of the partial factorisation method

The partial factorisation method has been used to obtain the global and regional signal components in the Ringhals measurements in the two operating points lying closest to the point where the limit cycle oscillations occurred. The global component is obtained directly as a result of the partial factorisation procedure through (52). However, determination of the regional mode is more difficult. This is because it is not given directly as an integral parameter such as the global component rather it is contained in all the calculated space-dependent components $\delta\Psi(\boldsymbol{r}_i, t)$. Moreover, in many of these signals the mode has a relatively low amplitude (weight).

Thus it is necessary to devise some averaging technique, similar to (52), to determine a reliable DR for the regional mode. Therefore, we suggest here a phase delay-corrected averaging of the signals $\delta\Psi(\boldsymbol{r}_i, t)$. The phase difference between each signal $\delta\Psi(\boldsymbol{r}_i, t)$ and a reference signal $\delta\Psi(\boldsymbol{r}_k, t)$ is determined at the resonance frequency and it is denoted by φ_{ki} . The out-of-phase behaviour of the signals is not perfect and deviations occur, but by using the procedure below such deviations are corrected for in the final result. In formulae, we have

$$\delta R_{av}(t) \;=\; \sum_{i\,=\,1}^{M} \frac{\delta\Psi(\boldsymbol{r}_i, t)}{\phi_0(\boldsymbol{r}_i)} \cdot \cos(\varphi_{ki}) \tag{60}$$

where the static flux $\phi_0(\boldsymbol{r}_i)$ is used as a weight function of the relative importance of the space-dependent signals. By using the above equation, the amplitude of the out-of-phase component is strongly amplified, while a strong reduction in amplitude is obtained for the local noise component and for the term in $\delta\Psi$, which is due to the approximation of the integral with sums.

Having obtained the two signals δP and δR_{av}, they can now be used to obtain a DR for the global and regional components, respectively. An analysis of the performance of the method was made, and for details we refer again to Ref. [9]. Regarding the actual determination of the DRs from the signals, three different methods were used similarly to [7] (see [7] for details). The different methods yield somewhat different results for the DRs, but the DRs for the different axial levels are consistent within the same measurement. The resulting DRs for the global component in both cases D and H were approximately 0.8. The regional components showed somewhat higher DRs of around 0.85. The obtained global DRs are also consistent with those reported in previous publications ([7] and [8]). The regional DRs are also relatively consistent, although somewhat lower, compared to the results for the regional DRs obtained by the subtraction method in [7], and further they are

also somewhat higher than the results of the subtraction method obtained in [8]. This shows that the partial factorisation method and the subsequent amplification of the regional component leads to reasonable, consistent results that are comparable to previous methods.

Stability monitoring is not the only possible application of the factorisation method and it may sometimes be useful to separate different noise components and not only at the frequency of a resonance. For example, in void transport measurements axial cross-correlation between detectors in the same string is used and the local component is the interesting one. Elimination of the global component will improve the linear dependence of the phase, as is demonstrated below in Fig. 8. This possibility has not been investigated before.

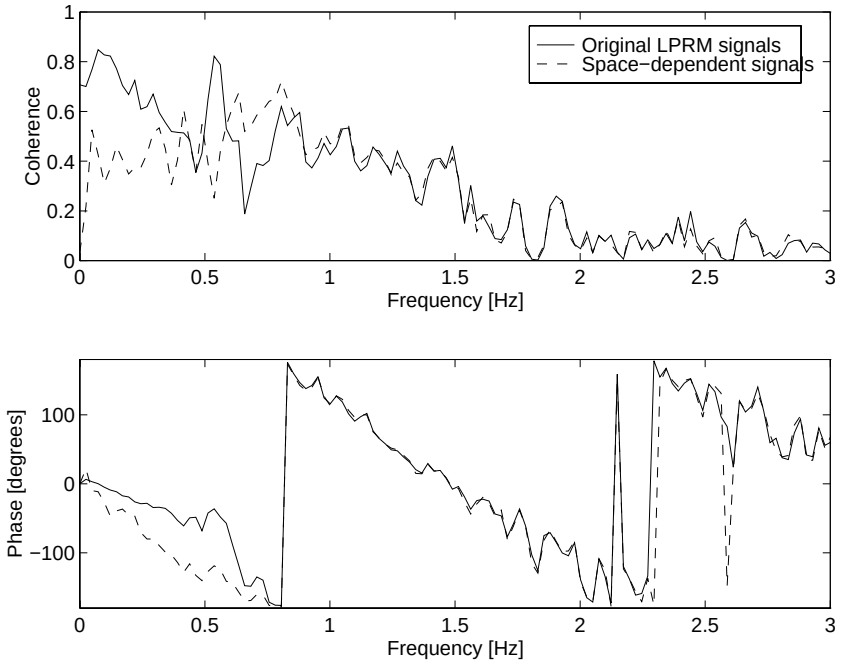

Fig. 8. Coherence (upper figure) and phase (lower figure) for the original and space-dependent signals in measurement D LPRM 20.

Fig. 8 shows the coherence and phase between LPRMs 20:2-20:4, i.e. LPRMs at axial levels 2 and 4 in string No. 20, respectively, in measurement D. The coherence of the raw (original) signals shows the usual broad-band character with some periodic dips, as a result of the interplay of the global and local components. Notice that in this case the global component is not equal to the global oscillation mode, which is present only at 0.5 Hz in the coherence of the original signal in Fig. 8, but rather it arises from a global component of white low-pass filtered background noise. Between 0 and 0.5 Hz, the magnitude of the coherence of the space-dependent component is much smaller than that of the original signal. This is because the global (reactivity) term is eliminated, only the local component remains in the space-dependent signal at these frequencies. At higher frequencies, on the other hand, the original and space-dependent signals have very similar coherence, showing that at these frequencies the global component has already diminished in the original signal. As was mentioned previously, the upward transport of void fluctuations leads to a linear phase φ as a function of frequency f (see Fig. 8). The slope of the phase φ yields the transport time τ_0, since $\varphi = 2\pi f \tau_0$. It is seen in Fig. 8 that the linear phase behaviour is

improved considerably at low frequencies by using the coherence between the space-dependent signals instead of the original signals. The effect of both the broad-band and the resonant global components is eliminated. This figure also illustrates the usefulness of the factorisation technique in areas other than determining stability properties. It has to be added that the component separation in this case cannot be achieved by the subtraction method, for quite obvious reasons. The factorisation technique is also applied in some further examples shown in [9].

3.5 Conclusions

It has been shown that with the partial factorisation procedure, i.e. using detectors lying in one radial plane (one axial elevation) only, the global and space-dependent components can be properly separated. A simple phenomenological model was introduced and by taking into account the approximate steps performed in the factorisation method, the success and failure of the present and previous versions of the method could be explained. Regarding BWR oscillations, the decay ratios of the global and the regional modes can be determined. A simple but somewhat improved method was elaborated for determining the amplitude $\delta R(t)$ of the regional (out-of-phase) oscillations from the space-dependent signals. Finally, we have shown an example of the application of the method also in measurements of the void transport time via correlations of detector signals.

Section 4

Investigation of the possibility of using the current and the flux gradient in core monitoring and diagnostics

4.1 Introduction

Generally, the neutron flux $\phi(\boldsymbol{r}, \underline{\Omega})$ is angularly dependent. However, in practice it is the scalar (angularly integrated) flux $\phi(\boldsymbol{r})$ that is used in both calculations and measurements. The angular dependence of the flux, or just the lowest order angular moment, the neutron current, or its diffusion theory approximation, the flux gradient, is not utilized. The reasons are relatively obvious; it is not easy to measure anything else than the scalar flux, and in calculations, such as criticality, burnup etc. it is still sufficient to use the scalar flux.

However, the situation is different in core monitoring and diagnostic problems. An anomaly is most often represented with a spatial discontinuity, such as a control or fuel rod surface or tip, around which the angular neutron flux is rather anisotropic. As a consequence, the neutron current, or the flux gradient, are expected to behave in a much more space dependent manner than the scalar flux in the vicinity of such objects of diagnostic interest. This is beneficial from the diagnostical point of view, since the spatial localisation of such perturbations or objects is always dependent on the space dependence of the flux or the noise. Even if the space dependence of the current is not stronger than that of the scalar flux, it represents additional information that is not available in the scalar flux, and thus can help in a diagnostic task.

Since, with current technology, the possibilities to construct angularly sensitive detectors or gradient detectors is much better than earlier, this possibility is quite promising. Thus we suggested to investigate the possible enhancements in core monitoring and diagnostics with the utilisation of the current or flux gradient, in both static and dynamic cases (noise diagnostic with current/gradient). A theoretical analysis of this possibility was performed and will be described here. A few selected model problems were investigated quantitatively. Through these model cases examples of possible applications are described.

4.2 General

Here we collect some definitions and formulae that will be used in the following. To facilitate the simplicity of description, one-group theory will be used throughout. All formulae can easily be generalized to many-group theory without any difficulty other than complications in the notations.

The neutron current, a vector quantity, is defined as the first angular moment of the angular flux:

$$\boldsymbol{J}(\boldsymbol{r}) = \int \underline{\Omega} \cdot \phi(\boldsymbol{r}, \underline{\Omega}) d\underline{\Omega} \tag{61}$$

With the scalar flux and the current, a two-term series expansion of the angular flux w.r.t.

angular moments is given as

$$\phi(\boldsymbol{r}, \underline{\Omega}) \cong \frac{1}{4\pi}[\phi(\boldsymbol{r}) + 3 \cdot \underline{\Omega} \cdot \boldsymbol{J}(\boldsymbol{r})] \tag{62}$$

In general, to calculate the current as defined by (61) requires the solution of the transport equation. In this paper one problem will be treated in which the true current is calculated, and this will be performed by Monte-Carlo methods.

Diffusion theory is an approximation to transport theory in which it is assumed that the angular flux is close to isotropic. In this approximation, the neutron current is given simply as the gradient of the scalar flux,

$$\boldsymbol{J}(\boldsymbol{r}) \; = \; -D(\boldsymbol{r}) \cdot \nabla\phi(\boldsymbol{r}) \tag{63}$$

In this approximation it is sufficient to solve the diffusion equation, which is much simpler than to solve the transport equation. Also, regarding measurement techniques, it is easier to construct a gradient detector than a current detector. The disadvantage of using the gradient is that close to strong inhomogeneities, such as control rods, reactor boundary etc., diffusion theory is rather inexact, and the gradient can be a quite bad approximation to the true current. Used with care, however, the gradient can be a very useful complement to the scalar flux.

In the dynamic case, a time-dependent neutron flux need to be used in the above definitions to obtain the time-dependent current and gradient. In the following we will only consider the fluctuations in the current in the diffusion theory approximation, i.e. the gradient noise. For simplicity we will call it a “current noise”. By the usual way of defining noise as deviations from the expected value, we write

$$\phi(\boldsymbol{r}, \underline{\Omega}, t) \; = \; \phi_0(\boldsymbol{r}, \underline{\Omega}) + \delta\phi(\boldsymbol{r}, \underline{\Omega}, t) \tag{64}$$

for the angular flux, where $\delta\phi(\boldsymbol{r}, \underline{\Omega}, t)$ is the angular noise. Likewise, the scalar and current noise are defined through

$$\phi(\boldsymbol{r}, t) \; = \; \phi_0(\boldsymbol{r}) + \delta\phi(\boldsymbol{r}, t) \tag{65}$$

and

$$\boldsymbol{J}(\boldsymbol{r}, t) \; = \; \boldsymbol{J}_0(\boldsymbol{r}) + \delta\boldsymbol{J}(\boldsymbol{r}, t) \tag{66}$$

Then, in the diffusion theory approximation, one obtains the time- or frequency dependent Fick’s law for the current noise, expressed as the gradient of the scalar noise:

$$\delta\boldsymbol{J}(\boldsymbol{r}, t) \; = \; -D \cdot \nabla\delta\phi(\boldsymbol{r}, t) \tag{67}$$

The value of the above expression is emphasized when using together with the usual expression of the scalar noise in the frequency domain, i.e.

$$\delta\phi(\boldsymbol{r}, \omega) = \int G(\boldsymbol{r}, \boldsymbol{r}', \omega) \cdot S(\boldsymbol{r}', \omega) d\boldsymbol{r}' \tag{68}$$

Combining with (67) gives

$$\delta \boldsymbol{J}(\boldsymbol{r}, \omega) = -D \int \nabla_r G(\boldsymbol{r}, \boldsymbol{r}', \omega) \cdot S(\boldsymbol{r}', \omega) d\boldsymbol{r}' \tag{69}$$

Eqn (69) expresses the fact that the current noise can be calculated through the gradient of the same transfer function as the one used for calculating the scalar noise. In all cases where there is an analytical formula available, this calculation can be performed in a straightforward way. Some examples will be given below.

In the examples below, we assume that one has access to a detector that can measure both the current and the scalar flux (abbreviated as a C/F detector). In other words, we assume that both the scalar flux and the current (gradient) are available in one single spatial point. We give some examples below how this information can be used in various localisation tasks. More details and examples can be found in Ref. 10.

4.3 Examples of application: static cases

Localisation of a point source

As the first application, it will be illustrated how a static point source in a purely moderating medium can be located in principle by a measurement in one single point. Again, as in the whole of this Section, one-group theory is used and we only deal with thermal sources and fluxes/currents.

Assuming a source at position $\boldsymbol{r}_0$, i.e.

$$Q(\boldsymbol{r}) = Q \cdot \delta(\boldsymbol{r} - \boldsymbol{r}_0) \ , \tag{70}$$

solution of the diffusion equation gives the scalar flux as

$$\phi(\boldsymbol{r}) = \frac{Q e^{-\frac{|\boldsymbol{r} - \boldsymbol{r}_0|}{L}}}{4\pi D |\boldsymbol{r} - \boldsymbol{r}_0|} \tag{71}$$

where L is the diffusion length, $L = (D/\Sigma_a)^{1/2}$

Finding the source position $\boldsymbol{r}_0$ by measuring the scalar flux only requires at least 4 traditional detectors at different spatial positions. However, since the neutron current has three vector components in 3 dimensions, the scalar flux and the current, as measured in just one point, is sufficient to locate the position of a source of unknown strength.

From (71) one obtains that

$$\boldsymbol{J}(\boldsymbol{r}) = -D \cdot \nabla\phi(\boldsymbol{r}) = D \frac{\boldsymbol{r} - \boldsymbol{r}_0}{|\boldsymbol{r} - \boldsymbol{r}_0|} \cdot \left(\frac{1}{L} + \frac{1}{|\boldsymbol{r} - \boldsymbol{r}_0|} \right) \cdot \phi(\boldsymbol{r}) \tag{72}$$

Eqn (72) shows that the vector $\boldsymbol{J}(\boldsymbol{r})$ points into the direction $\boldsymbol{r}-\boldsymbol{r}_0$. This means that drawing a line from $\boldsymbol{r}$ in the direction of $-\boldsymbol{J}(\boldsymbol{r})$, the unknown source position $\boldsymbol{r}_0$ will lie on this line. In other words, measuring the current in one point alone shows the direction where the source is located. Although such a simple relationship is only due to the simplicity of the situation, namely a homogeneous infinite system, the directional selectivity of the measured current is always present, although in a somewhat more indirect way.

The remaining parameter, the distance $|\boldsymbol{r}-\boldsymbol{r}_0|$, can be determined by using the scalar flux and $\boldsymbol{J}(\boldsymbol{r})$ together. From (72) one obtains

$$\frac{|\boldsymbol{J}(\boldsymbol{r})|}{\phi(\boldsymbol{r})} = D\left(\frac{1}{L}+\frac{1}{|\boldsymbol{r}-\boldsymbol{r}_0|}\right) \tag{73}$$

Thus from $\boldsymbol{J}(\boldsymbol{r})$ and $\phi(\boldsymbol{r})$ the distance $|\boldsymbol{r}-\boldsymbol{r}_0|$ can be obtained by inverting (73), see also Fig. 9. The Figure also shows that if $|\boldsymbol{r}-\boldsymbol{r}_0|$ is much larger than the diffusion length L, the ratio $|\boldsymbol{J}_r|/\phi$ becomes insensitive to $|\boldsymbol{r}-\boldsymbol{r}_0|$, which thus cannot be determined. Pointing out the direction

$$\frac{\boldsymbol{r}-\boldsymbol{r}_0}{|\boldsymbol{r}-\boldsymbol{r}_0|}$$

from (72) does however not suffer from this fact.

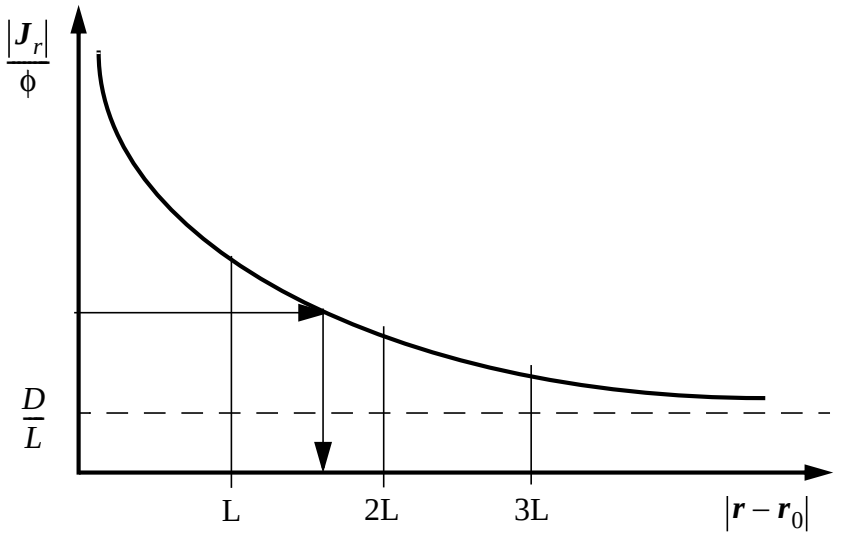

Fig. 9. Dependence of the current to flux ratio on the distance from the source.

The above illustrates the fact that the spatial range within which source localisation and other diagnostics can be performed by one current + flux (C/F) detector is more limited than it would be if the same task is to be performed with, say, three or four flux detectors, placed at suitable distances from each other and the source. However, in some cases there may be only one detector position available in a localisation task close enough to the source. One such example is treated below. Then, use of the current and the flux together is the only chance to perform the diagnostics.

Diagnostics of control rods and control rod pins

The second application concerns the diagnostics of either whole control rod rods or individual control pins. Regarding complete control rods, some attention was paid recently

to the possibility of determining the axial position of a control rod from the axial flux shape in the vicinity of the rod (Ref. [11]). In the above reference, the information in the distortion of the axial flux profile was used, in combination with a neural network technique, to determine the rod elevation. Due to the strong perturbation that a black absorber represents in a core, it can be expected that the distortion in the axial dependence of the current vector, becomes much more characteristic than that of the scalar flux. In this case, we refer to the exact (transport theory definition) of the current, and not its diffusion approximation (flux gradient), since in such cases diffusion theory does not give adequate results.

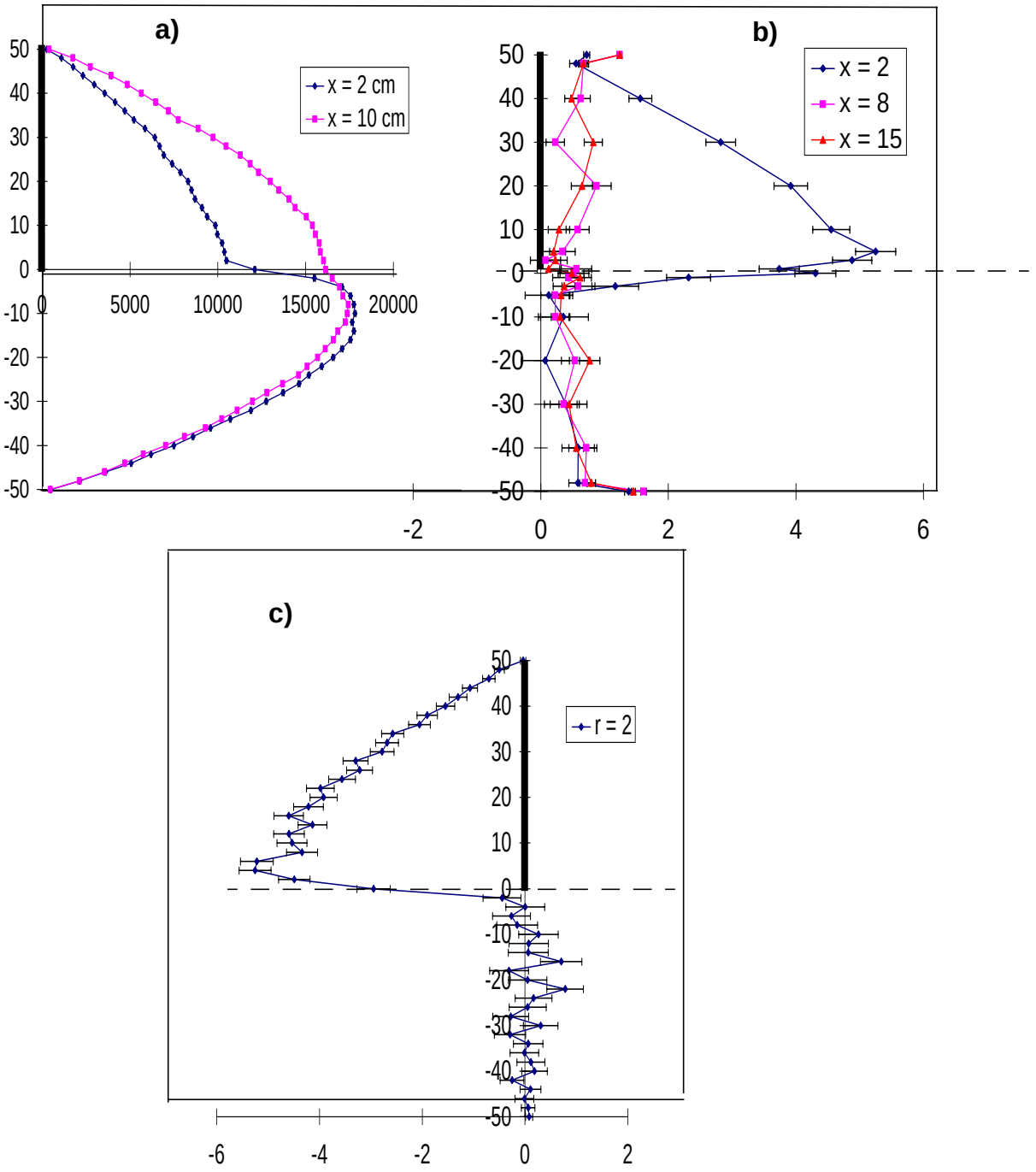

Fig. 10. The axial dependence of the flux and the current close to a partially inserted control rod in a 3-D cylindrical reactor, calculated by Monte Carlo (from Ref 12). a) scalar flux; b) absolute value of the current; c) radial component of the current. The numbers in the boxes represent radial distance from the rod.

Fig. 10. demonstrates that there is much more explicit information available on the rod position in the current than in the scalar flux. In all three diagrams in the Figure the rod is inserted to the middle of the reactor (y = 0). Figs. 10b and 10c show that in these cases one could make a quite good quantitative guess of the rod position from the measured data, whereas the same estimate would be more uncertain from the flux data. The calculations shown here were made by a Monte Carlo code in a 3-D cylindrical reactor, in order to obtain the true current (Ref. [12]).

In the static control rod diagnostic case, the use of the current can be extended from axial dependence to the radial dependence as well. This is the case when the radial (azimuthal) position of the control rod is also an unknown. Such is the case if static failures of a single control rod pin (finger) are to be diagnosed in a Westinghouse-type PWR. Fig. 11 serves for an illustration. Assume that one single control rod pin, or some section thereof, breaks down and falls to a lower position. The flux and the current will be influenced by this change and thus there is in principle a possibility to both detect such an event and identify the failed pin. However, due to the weakness of such a perturbation, the flux and current distortion can most likely not be detected outside the fuel assembly in question, not even in a neighbouring assembly position. Thus the only possibility is to use a current/flux detector within the assembly. If a complete mapping of the axial dependence of the scalar flux and the current vector is performed by a movable detector, then there is a chance that both the axial and the radial position of such a failed control rod finger can be determined. We do not have any simulated data to support this statement at present, but the problem can be studied via Monte-Carlo simulation and this is planned in future work.

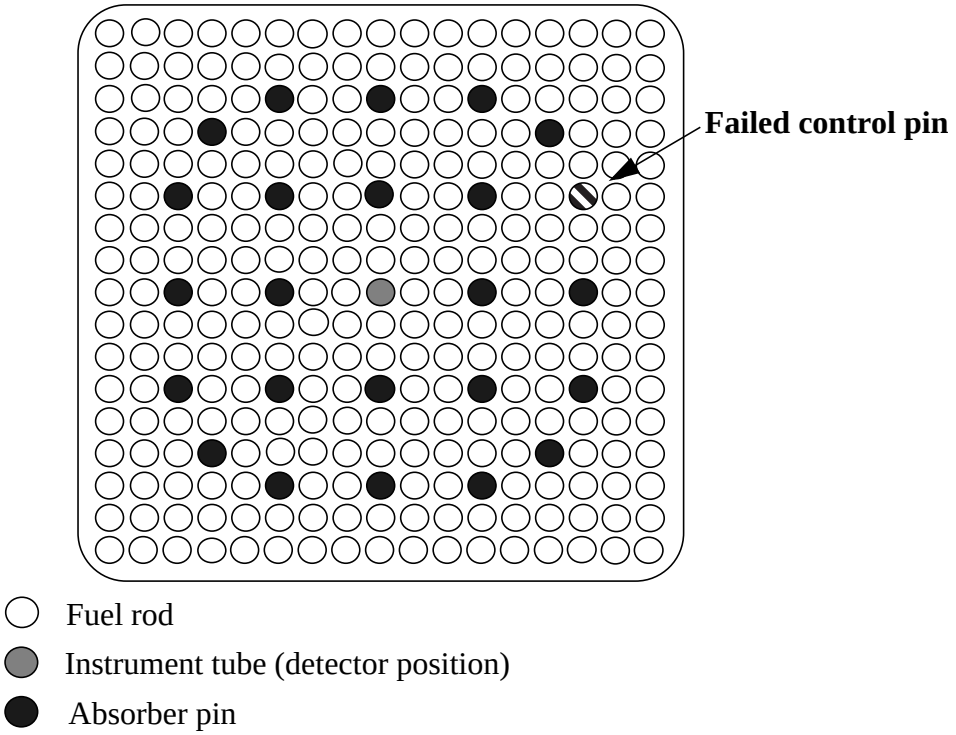

Fig. 11. Horizontal cross section of a PWR fuel assembly, containing a control rod and an instrument tube for a movable detector

4.4 Applications in dynamical cases

Here we only discuss the possibility of using the current or gradient noise, together with the scalar noise, to locate a vibrating control rod or control rod pin. Another example, the case of localisation of a point source of oscillating strength in an infinite, non-multiplying medium, is described in Ref. [10].

The task of locating the position of a vibrating control rod from the neutron noise was treated in earlier applications by using three neutron detectors at the same axial elevation but at different radial positions (triangulation). Due to axial homogeneity, this is a 2-D problem, and the task is to determine the rod position on the 2-D horizontal cross-section of the reactor. The static rod is described by the absorption cross-section

$$\Sigma_a^{rod} = \gamma \cdot \delta(\boldsymbol{r} - \boldsymbol{r}_p) \tag{74}$$

where γ stands for the rod strength and $\boldsymbol{r}_p$ is the static rod position. The vibrating rod is represented by

$$\Sigma_a^{rod} = \gamma \cdot \delta(\boldsymbol{r} - \boldsymbol{r}_p - \underline{\varepsilon}(t)) \tag{75}$$

where $\underline{\varepsilon}(t)$ is a 2-D displacement vector describing the stochastic rod trajectory during vibration. Thus the perturbation represented by the rod vibrations are given as

$$\delta\Sigma_a^{rod}(\boldsymbol{r}, t) = \gamma \cdot [\delta(\boldsymbol{r} - \boldsymbol{r}_p - \underline{\varepsilon}(t)) - \delta(\boldsymbol{r} - \boldsymbol{r}_p)] \tag{76}$$

As described in the previous works, with the above perturbation, the induced neutron noise can be written as

$$\delta\phi(\boldsymbol{r}, \omega) = \frac{\gamma}{D}\{G_{x_p}(\boldsymbol{r}, \boldsymbol{r}_p, \omega) \cdot \varepsilon_x(\omega) + G_{y_p}(\boldsymbol{r}, \boldsymbol{r}_p, \omega) \cdot \varepsilon_y(\omega)\} \tag{77}$$

Here,

$$G_{x_p}(\boldsymbol{r}, \boldsymbol{r}_p, \omega) \equiv \frac{\partial}{\partial x'}\{G(\boldsymbol{r}, \boldsymbol{r}', \omega) \cdot \phi(\boldsymbol{r}')\}\Big|_{\boldsymbol{r}' = \boldsymbol{r}_p} \tag{78}$$

and similarly for $G_{y_p}(\boldsymbol{r}, \boldsymbol{r}_p, \omega)$.

Since the vibration components $\varepsilon_x(\omega)$ and $\varepsilon_y(\omega)$ are also unknown, one needs at least 3 neutron detectors at positions $\boldsymbol{r}_1$, $\boldsymbol{r}_2$ and $\boldsymbol{r}_3$. Then, the neutron noise measured at these positions is expressed by 3 equations of the type (77). Two of them can be used to eliminate ε_x and ε_y in the third, and thus to create an identity called the “localisation equation”. This latter is a transcendental equation which contains the unknown rod position as its root. Alternatively, neural network methods can be used to train a network to identify the rod position from 3 neutron noise signals and using the direct expressions for the noise in the form of (77).

In this 2-D problem, the current and the current noise are 2-D vectors. Hence, together with the scalar noise, one current/flux (C/F) noise measurement serves 3 independent quantities just as in the case of 3 neutron noise detectors. In formulae, one C/F detector yields the measurement of the following 3 quantities:

$$\delta\phi(\boldsymbol{r}, \omega) = \frac{\gamma}{D}\{G_{x_p}(\boldsymbol{r}, \boldsymbol{r}_p, \omega) \cdot \varepsilon_x(\omega) + G_{y_p}(\boldsymbol{r}, \boldsymbol{r}_p, \omega) \cdot \varepsilon_y(\omega)\} \tag{79}$$

$$\delta J_x(\boldsymbol{r}, \omega) = -\gamma\{G_{xx_p}(\boldsymbol{r}, \boldsymbol{r}_p, \omega) \cdot \varepsilon_x(\omega) + G_{xy_p}(\boldsymbol{r}, \boldsymbol{r}_p, \omega) \cdot \varepsilon_y(\omega)\} \tag{80}$$

$$\delta J_y(\boldsymbol{r}, \omega) = -\gamma\{G_{yx_p}(\boldsymbol{r}, \boldsymbol{r}_p, \omega) \cdot \varepsilon_x(\omega) + G_{yy_p}(\boldsymbol{r}, \boldsymbol{r}_p, \omega) \cdot \varepsilon_y(\omega)\} \tag{81}$$

Here,

$$G_{xx_p} = \frac{\partial^2}{\partial x \partial x_p} G(\boldsymbol{r}, \boldsymbol{r}_p, \omega)\phi(\boldsymbol{r}_p) \tag{82}$$

etc.

Eqns (79) - (81) contain the same amount of independent information on ε_x, ε_y and $\boldsymbol{r}_p$ and can be used to construct a localisation procedure as was the case with $\delta\phi(\boldsymbol{r}, \omega)$ measured at three different positions. With a C/F noise detector at one single point, the diagnostics of a vibrating rod, in particular its localisation, is possible. This may be especially useful in case of the failure of a single control rod pin, as it was discussed in the static case, see also Fig. 11. The neutron noise induced by the vibration of one single control pin is not likely to be determined outside the assembly in which the pin is located, because at such distances the amplitude of the noise induced by the vibrations will be smaller than the background noise or noise from other sources. Thus it is essential to perform the diagnostics by using one single measurement position, close to the perturbation. The use of a C/F detector is again a promising possibility to achieve this.

4.5 Conclusions

It is planned that the feasibility of the use of the current will be investigated experimentally in further work. Regarding possible hardware development, both fibre-based scintillation detectors as well as SPN detectors can be developed into current or gradient detectors. In order to achieve applicability in practice, a number of problems need to be investigated and solved, both experimentally and conceptually. However, the potential of the method is quite promising, which justifies further work in this field.

Plans for the continuation

In Stage 5 we plan to include the following parts in the current R&D program:

- Continued investigation of the possibilities of using the flux gradient for diagnostics: study of a detector and Monte-Carlo calculations. A new type of thin neutron detector, based on an optical fibre whose tip consists of a lithium or thorium loaded scintillator, has been developed in Japan. This detector has a spatial resolution of ~1 mm. We have received this new technology and also made some preliminary tests. In order to evaluate the properties of this new detector, we plan to perform some measurements with a neutron source. We also plan to make comparisons between the measurement results and Monte-Carlo calculations using the code MCNP.
- Comparative investigation of the problem of localization of vibrating control-rods using ordinary noise and "current" noise. In Stage 4, we described how a vibrating absorber can be localized using measurements of the neutron noise and fluctuations of the flux gradient ("current noise"). A quantitative investigation of this method is proposed using simulated (calculated) noise signals.
- Calculation of the transfer function in a 2-region system using 2-group theory. The transfer function has hitherto only been calculated in 2-D bare systems using 1-group diffusion theory. Two-group theory is necessary to describe reflected systems as well as the so called local component of the neutron noise, which exists 1-2 diffusion lengths from the source. In Stage 5, we plan to derive and calculate the complex transfer function for a 2-D cylindrical, reflected reactor. The local instability event in Forsmark 1, where the disturbance is located close to the reflector, confirmed the need for such a transfer function.
- Development of the theory of zero reactor noise with the purpose of using it to reactivity measurements. Fluctuations in the number of detector pulses during start-up, i.e. for a subcritical core with a source, have been used to measure reactivity for many decades. In these methods, either the relative variance (Feynman-alpha method) or the correlations (Rossi-alpha) are measured as functions of time. By comparison with theoretical expressions for the same quantities, the reactivity can be determined by curve fitting. The development we suggest here concerns the use of "multiple" start-up sources, such as a Cf-252 source, instead of the traditional Am-Be or Pu-Be source. The difference is that the traditional sources emit only one neutron at a time, and have thus Poisson statistics. Multiple sources emit several correlated neutrons, and this fact enhances the effectivity of the method. However, the theoretical formulas used so far in the evaluation are all based on Poisson sources. We propose to elaborate the theory of Feynman-alpha and Rossi-alpha measurements for multiple sources and to derive the Feynman-alpha and Rossi-alpha formulae for such cases. In the first stage, similarly to all traditional work in the literature, space-independent stochastic theory will be used. However, at a later stage also space-dependent effects will be investigated through Monte-Carlo simulations. Space-dependent effects have relevance in the interpretation of some events (deviations between measured and true reactivity) that have occurred during start-up at operating reactors.

Acknowledgement

This project was supported by the Swedish Nuclear Power Inspectorate, contract No. 14.5-970583-97200.

References

[1] Pázsit I. and Garis N. S. “Forskningsprogram angående härddiagnostik med neutronbrusmetoder.” *Etapp 1. Slutrapport, SKI Rapport* 95:14 (1995)

[2] Pázsit I., Garis N. S. and Thomson O. “Forskningsprogram angående härddiagnostik med neutronbrusmetoder.” *Etapp 2. Slutrapport, SKI Rapport* 96:50 (1996)

[3] Pázsit I., Garis N. S., Karlsson J., Rácz A. “Forskningsprogram angående härddiagnostik med neutronbrusmetoder.” *Etapp 3. Slutrapport, SKI Rapport* 97:31 (1997)

[4] Karlsson J. K-H. and Pázsit I. “An Analytically Solvable, Axially Non-homogeneous Reactor Model. I. General Solutions”,To appear in *Ann. Nucl. Energy* (1998)

[5] Karlsson J. K-H. and Pázsit I. An Analytically Solvable, Axially Non-homogeneous Reactor Model. II. Reactor kinetic approximations. Submitted to *Ann. nucl. Energy* (1998)

[6] Garis N. S. and Pázsit I., “Application of static codes for determination of the neutron noise using adiabatic approximation”, Unpublished (1997)

[7] van der Hagen T. H. J. J., Pázsit I., Thomson O. and Melkersson B., “Methods for the Determination of the In-phase and Out-of-phase Stability Characteristics of a Boiling Water Reactor”, *Nuclear Technology* Vol. **107**, 193-214 (1994)

[8] Johansson A., “OECD/NEA BWR Stability Benchmark. Evaluation of Decay Ratio for Ringhals unit 1 cycle 14, 15, 16 and 17”, Vattenfall Ringhals report 0470/95 (1995)

[9] Karlsson J. and Pázsit I. “Noise decomposition in BWRs with application to stability monitoring”, To appear in *Nucl. Sci. Engng*. (1998)

[10] Pázsit I. On the possible use of the neutron current in core monitoring and diagnostics. *Ann. nucl. Energy* **24**, 1257 - 1270 (1997)

[11] Garis N. S., Pázsit I., Sandberg U. and Andersson T., “Determination of PWR control rod position by core physics and neural network methods”, To appear in *Nucl. Technology* (1998)

[12] Karlsson J. K-H. and Lindén P. (1997) Monte Carlo simulation of neutron transport in a homogeneous reactor with a partially inserted control rod. Chalmers internal report CTH-RF-130.